

## Effects of Lightning Punctures on the Core-Shield Voltage of Buried Cable

By S. G. UNGAR

(Manuscript received August 28, 1979)

*A common form of lightning-induced cable damage occurs when a lightning surge travels down the shield of a cable, inducing large voltages between the cable core and the shield and leading to possible insulation breakdown and arcing. The magnitude of this core-shield voltage is a function of how quickly the lightning current is shunted to the surrounding soil, either through a ground or by puncturing the protective jacket of the cable. Core-shield voltages are calculated for various combinations of cable length, cable diameter, soil conductivity, lightning pulse shape, and resistance of the cable jacket to puncturing and compared with results obtained by assuming that the cable jacket is punctured along its entire length. This latter assumption, the "bare shield" model, has generally been used to predict core-shield voltages. We have found that the "bare shield" model can lead to a significant underestimation of the core-shield voltage, particularly for small diameter cables with long distances between grounds (on the order of 10 kilometers). We present curves that provide an estimate of the peak core-shield voltage for a cable in which the jacket punctures for a portion of its length.*

### I. INTRODUCTION

A common form of lightning-induced cable damage occurs when a lightning surge travels down the shield of a cable. Under certain conditions, this lightning current may develop very large voltages between the shield and the core conductors leading to possible insulation breakdown and arcing. It is therefore of interest to determine the range of core-shield voltages that can be expected for a cable exposed to lightning under various circumstances. We confine our discussion in this paper to buried cable.

A lightning surge "enters" a cable either directly by puncturing the cable jacket, by sparking across a protective gap, or by induction. The

lightning current then splits and travels along the shield in both the positive and negative  $x$  directions (Fig. 1). These surges have a rise time on the order of microseconds and considerably slower fall times on the order of tens of microseconds. The peak value of the surge is on the order of tens of kiloamperes. For the purpose of analysis, we assume that the surge is a double exponential, and we characterize it by giving its peak value, its rise time (in microseconds), and its fall time (in microseconds). Thus, a typical pulse might be identified as a 10 kA,  $7.5 \times 65$  surge, meaning a double-exponential pulse of peak value 10 kA, with a 7.5-microsecond rise time and 65-microsecond time to half value (see Fig. 2).

If the surge is large enough, as it travels along the cable shield it punctures the jacketing insulation.<sup>1</sup> A large part of the lightning current leaks off the shield through these punctures; in effect, the cable shield is then in electrical contact with the ground. At some point, so much current has leaked off that not enough is left to cause puncturing; what remains then travels along the shield, confined by the highly resistive polyethylene jacket.

The behavior of a lightning pulse on the shield of a buried cable can be rigorously described by use of electromagnetic field equations. We use a simpler model developed by Sunde<sup>2</sup> in which the current is assumed to travel on a transmission line consisting of the cable shield and the earth. If one can deduce the parameters of this transmission

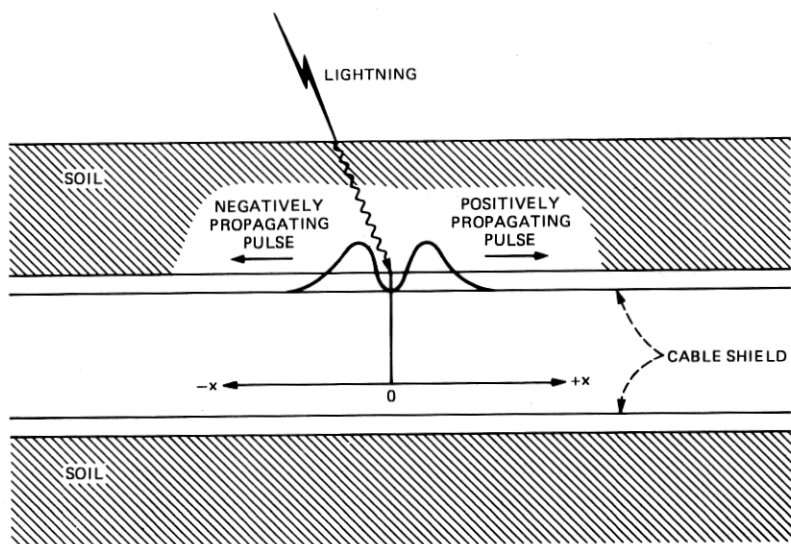


Fig. 1—Buried cable configuration.

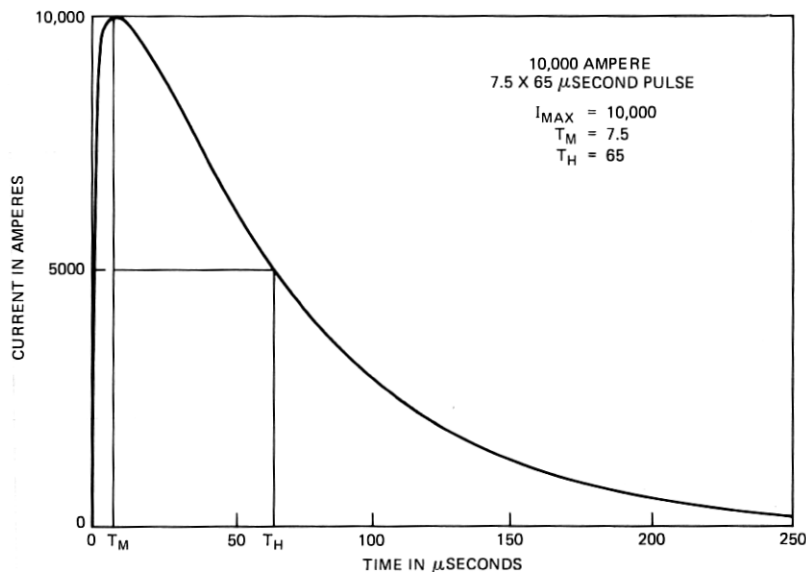


Fig. 2—Double exponential pulse.

line, the standard transmission line equations may be used to describe the behavior of the current surge. The cable also has a core of insulated wire pairs and these pairs, taken together as a "single" conductor along with the shield, constitute another transmission line. This core-shield transmission line is coupled to the shield-earth transmission line, the coupling parameter being the transfer impedance of the shield. The result of this coupling is that, as the current in the shield-earth transmission line travels down the line, a voltage develops between the core conductors and the shield. For a typical lightning surge, this voltage may become quite large, on the order of 10 kV, which may be enough to damage the insulation on the core conductors. The voltage reaches its greatest value at the entry point of the lightning current, and is a function of the shield transfer impedance, the lightning current magnitude, and the distance along the cable that the current travels before it is removed to earth.

It is this last factor that complicates the analysis, since the distance the current travels on the cable shield is controlled to a great extent by the ability of the current to puncture the jacket. In the region where the current is large and punctures the jacket, the shield-earth transmission line has characteristics typical of a "bare" cable i.e., a cable without an outer jacket; in the region in which the current has become too weak to puncture the jacket, the shield-earth transmission line has characteristics corresponding to an insulated cable.

To simplify calculations, it has often been assumed that the lightning pulse punctures the jacket for the entire length of the cable; this is a good assumption if the discussion is confined to large pulses and short cables. In this study, we have attempted to take into account the nonlinear behavior of the cable jacket in computing the core-shield voltage; we have found that including this behavior and assuming that the jacket is not punctured for the entire length of the cable can lead to a significant increase in the core-shield voltage, particularly for cables with long distances between grounds (on the order of 10 kilometers).

## II. THE SHIELD-EARTH TRANSMISSION LINE

We assume that a lightning surge introduced to the shield of a buried cable behaves as if the cable shield and the earth constitute the two conductors of a linear, homogenous transmission line. One can then use standard transmission line equations to describe the behavior of the pulse. If we characterize the pulse  $I(x, t)$  by its frequency spectrum  $I(x, \omega)$ , we may write

$$I(x, \omega) = I(0, \omega)e^{-\Gamma x}. \quad (1)$$

In the above,  $t$  is time,  $x$  is distance along the line, and  $\omega$  is frequency in radians/second. The propagation constant of the line is  $\Gamma$ , and in general it is a complex number whose real part  $\alpha$  gives the attenuation/length and whose complex part  $\beta$  gives the phase shift/length.

We assume that the line is terminated at  $x = 0$  in an infinite impedance, so that the line may be neglected for negative values of  $x$  (this is equivalent to writing  $I(x, \omega) = I(-x, \omega) = I_{\text{lightning}}/2$ ). Furthermore, eq. (1) assumes that no reflections are on the line. For most situations with which we will be concerned, this is a valid approximation: In the case of a cable punctured over its entire length, reflections are unimportant because the attenuation is so great. In the instance that the lightning current is so small that the cable insulation does not puncture at all, reflections are important only if the cable is terminated at its far end in an impedance very different from the characteristic impedance of the shield-earth transmission line; we show in Section VII that the effect of these reflections may be easily accounted for. If the pulse is in the range in which the jacket punctures for part of the length of the cable, reflections from the punctured-intact transition may become a significant factor; this case is dealt with in detail in Section III.

The propagation constant is related to the impedance/length  $Z(\omega)$  and the admittance/length  $Y(\omega)$  by the expression

$$\Gamma^2(\omega) = Z(\omega)Y(\omega). \quad (2)$$

For the shield-earth transmission line, we may write (Ref. 1 and Ref. 2, Ch. 5)\*

$$Y(\omega) = \left[ Y_i^{-1} + \frac{1}{\pi((1/\rho) + j\omega\epsilon)} \ln \frac{1.12}{\Gamma \hat{a}} \right]^{-1} \quad (3)$$

$$Z(\omega) = Z_i + \frac{j\omega\mu}{2\pi} \ln \frac{1.85}{\hat{a}(\gamma^2 + \Gamma^2)^{1/2}} \quad (4)$$

$$\hat{a} = \sqrt{a_o^2 + 4d^2} \quad (5)$$

$$\gamma^2 = j\omega\mu \left( \frac{1}{\rho} + j\omega\epsilon \right), \quad (6)$$

where

$\omega$  = frequency [radians/sec]

$\mu$  = permeability of soil [henries/meter]

$\rho$  = resistivity of soil [meter-ohms]

$\epsilon$  = permittivity of soil [farads/meter]

$\hat{a}$  = effective radius of shield [meters]

$a_o$  = outer radius of shield [meters]

$d$  = depth of cable [meters]

$Z_i$  = external impedance with external return of hollow cylinder [ohms/meter]

$Y_i$  = admittance/length of cable jacket [mhos/meter].

An expression for  $Z_i$  is given by Schelkunoff:<sup>1,3</sup>

$$Z_i = \frac{\eta}{2\pi a_o} \left[ \coth \sigma t_s + \frac{1}{8\sigma} \left( \frac{3}{a_i} + \frac{1}{a_o} \right) \right], \quad (7)$$

where

$$\eta = \frac{\sigma}{g_s} \quad (8)$$

$$\sigma^2 = j\omega g_s \mu_s \quad (9)$$

and

$g_s$  = conductivity of shield [mhos/meter]

$\mu_s$  = permeability of shield [henries/meter]

$t_s$  = thickness of shield [meters]

$a_i = a_o - t_s$  = inner radius of shield [meters].

\* In eqs. (3) and (4), the factors 1.12 and 1.85 result from the use of small-argument approximations for Bessel functions.

The admittance/length of the jacket,  $Y_i$ , is easily derived:

$$Y_i = \frac{2\pi}{\ln(a_{co}/a_{ci})} (g_c + j\omega\epsilon_c), \quad (10)$$

where

- $a_{co}$  = outer radius of jacket [meters]
- $a_{ci}$  = inner radius of jacket [meters]
- $g_c$  = conductivity of jacket [mhos/meter]
- $\epsilon_c$  = permittivity of jacket [farads/meter].

These equations are valid from dc to about  $10^7$  Hertz, at which point approximations to Bessel functions used to derive (3), (4), and (7) break down.<sup>1,2</sup>

Putting (3) and (4) into (2), we obtain an equation for  $\Gamma(\omega)$ :

$$\Gamma^2(\omega) = \frac{Z_i + (j\omega\mu/2\pi)\ln(1.85/\hat{a}(\gamma^2 + \Gamma^2)^{1/2})}{Y_i^{-1} + \pi((1/\rho) + j\omega\epsilon)\ln(1.12/\Gamma\hat{a})}. \quad (11)$$

Solution of this nonlinear, complex, transcendental equation gives  $\Gamma$  as a function of frequency. Putting the solution for  $\Gamma$  into eqs. (3) and (4) gives  $Y$  and  $Z$ . Thus the characteristics of the shield-earth transmission line may be determined, and the behavior of the lightning pulse obtained by solution of eq. (1).

### III. THE CORE-SHIELD VOLTAGE

#### 3.1 Development of $V_{cs}$ equations

Sunde's analytical development (Ref. 2, Chapter 9) shows that the entry point voltage developed between the core conductors and the shield when a pulse travels down the shield is given by

$$V_{cs}(0, \omega) = \int_0^{\infty} I(0, \omega) Z_s e^{-(\Gamma + \Gamma_0)x} dx, \quad (12)$$

where

$V_{cs}$  = core-shield voltage [volts]

$I(0, \omega)$  = current at entry point, traveling in the positive  $x$  direction  
(half the total lightning current) [amperes]

$Z_s(\omega)$  = shield transfer impedance [ohms]

$\Gamma(\omega)$  = shield-earth propagation constant given by eq. (11) [meters<sup>-1</sup>]

$\Gamma_0(\omega)$  = core-shield propagation constant [meters<sup>-1</sup>].

Here  $\Gamma_0$  may be written as

$$\Gamma_0 = \left[ -\frac{\omega^2}{v_0^2} + j\omega C_0 R_0 \right]^{1/2}, \quad (13)$$

where

$v_0$  = phase velocity of core-shield transmission line [meters/second]

$C_0$  = capacitance/length of core-shield transmission line [farads/meter]

$R_0$  = resistance/length of core-shield transmission line  $\cong R_s$ , resistance/length of shield [ohms/meter].

The internal surface impedance with external return of a hollow cylinder is  $Z_s$  (also known as the transfer impedance), and is given by Schelkunoff.<sup>3</sup>

$$Z_s = \frac{\eta}{2\pi\sqrt{a_i a_o}} \operatorname{csch} \sigma t_s, \quad (14)$$

where  $\eta$  and  $\sigma$  are given by (8) and (9), and the other symbols are as defined above. At low frequencies,  $Z_s$  is very nearly equal to  $R_s$ , the dc resistance of the shield.

Equation (12) applies to an infinitely long cable. If the cable terminates at a distance  $x_d$ , the limit on the integral changes and (12) becomes

$$V_{cs}(0, \omega) = \int_0^{x_d} I(0, \omega) Z_s e^{-(\Gamma + \Gamma_0)x} dx, \quad (15)$$

where the effect of reflections at the termination have been neglected.

We are interested in evaluating (15) for various values of  $\Gamma$ .

If a lightning surge on a cable is greater than a minimum threshold value  $I_{th}$ , it will cause the cable jacket to puncture. As mentioned above, when the jacket punctures, the shield-earth transmission line behaves as if the shield were in direct contact with the earth.<sup>1</sup> We denote the propagation constant in this "bare" case  $\Gamma_B$ . If the surge is too small to puncture the jacket, i.e.,  $I < I_{th}$ , the cable behaves as if it were well insulated (which it is). We then call the propagation constant  $\Gamma_I$ . Let us examine the possible behavior mechanisms of a lightning pulse along a length  $x_d$  of polyethylene-insulated cable.

In the first instance, consider a pulse in which the current at  $x = 0$  is less than the threshold current. In this case, the jacket will not puncture and the lightning pulse travels along the shield in accordance with eq. (1), with  $\Gamma = \Gamma_I$ . Setting  $\Gamma = \Gamma_I$  in (15) and integrating, we get

$$V_{cs}(0, \omega) = \frac{I(0, \omega) Z_s}{\Gamma_I + \Gamma_0} [1 - e^{-(\Gamma_I + \Gamma_0)x_d}]. \quad (16)$$

Now consider a lightning pulse which is large enough to puncture the jacket. The pulse will now propagate down the shield in accordance with (1), with  $\Gamma = \Gamma_B$ . As the pulse travels, it gets smaller as current leaks off into the earth, the attenuation rate being given by  $\alpha$ , the real part of  $\Gamma$ . At some distance from the entry point, the pulse will become too weak to continue puncturing the jacket. From this point on, the pulse propagates as if  $\Gamma = \Gamma_I$ , the insulated case.

We must now consider two possibilities: If the pulse is large it will have to travel a long distance before it stops puncturing. Let us call this distance  $x_{th}$ . If  $x_{th}$  is greater than  $x_d$ , the cable behaves as if it were bare for its entire length. We may then set  $\Gamma = \Gamma_B$  in (15), and integrate:

$$V_{cs}(0, \omega) = \frac{I(0, \omega)Z_s}{\Gamma_B + \Gamma_0} [1 - e^{-(\Gamma_B + \Gamma_0)x_d}]. \quad (17)$$

The second possibility to consider is that the pulse stops puncturing before it reaches the end of the cable, i.e.,  $x_{th} < x_d$ . The cable now behaves differently over different portions of its length. From  $x = 0$  to  $x = x_{th}$ , the lightning punctures the jacket and the cable behaves as if it were bare,  $\Gamma = \Gamma_B$ ; from  $x = x_{th}$  to  $x = x_d$  the pulse is too weak to puncture the jacket, and the cable behaves as if it were insulated,  $\Gamma = \Gamma_I$ . As the pulse travels along the cable, it first experiences a zone of punctured jacket and then a zone of insulated jacket. If the transition between these zones is assumed to be abrupt, part of the pulse will be reflected back to the punctured section, and part will be transmitted through the boundary to the insulated section. If we neglect multiple reflections in the punctured zone and if we assume that the insulated section is either very long or terminated in an impedance approximately equal to its characteristic impedance, eq. (15) may be written

$$V_{cs}(0, \omega) = Z_s \left[ \int_0^{x_{th}} I(0, \omega) e^{-(\Gamma_B + \Gamma_0)x} dx \right. \\ \left. + \rho_i \int_0^{x_{th}} I(x_{th}, \omega) e^{(\Gamma_B + \Gamma_0)(x - x_{th})} dx \right. \\ \left. + (1 + \rho_i) \int_{x_{th}}^{x_d} I(x_{th}, \omega) e^{-(\Gamma_I + \Gamma_0)(x - x_{th})} dx \right], \quad (18)$$

where  $\rho_i$  is the reflection coefficient.

The first term represents the voltage due to the current pulse propagating along the punctured section of cable, the second term is a result of the current reflected from the boundary at  $x_{th}$ , and the third term is due to the current transmitted across the boundary that travels along the insulated section. The reflection coefficient  $\rho_i$  may be written



$$\rho_i = \frac{Z_{oB} - Z_{oI}}{Z_{oB} + Z_{oI}}, \quad (19)$$

where

$Z_{oI}$  = characteristic impedance of the insulated portion of the cable

$Z_{oB}$  = characteristic impedance of the punctured portion of the cable

and, in general,

$$Z_o = \sqrt{\frac{Z(\omega)}{Y(\omega)}}.$$

From eq. (1),

$$I(x_{th}, \omega) = I(0, \omega)e^{-\Gamma_B x_{th}}. \quad (20)$$

Putting (20) into (18), integrating and collecting terms,

$$V_{cs}(0, \omega) = I(0, \omega)Z_s \left\{ \frac{(1 + \rho_i e^{-\Gamma_B x_{th}})(1 - e^{-(\Gamma_B + \Gamma_0)x_{th}})}{\Gamma_B + \Gamma_0} + (1 + \rho_i) \frac{e^{-\Gamma_B x_{th}} [1 - e^{-(\Gamma_I + \Gamma_0)(x_d - x_{th})}]}{\Gamma_I + \Gamma_0} \right\}. \quad (21)$$

The characteristic impedance of the punctured section is generally very different from that of the insulated section, and the reflection coefficient, especially for low frequencies, is very close to  $-1$ . Equation (21) would seem to predict that the contribution to the core-shield voltage from the insulated section of line should be very small because of the factor  $(1 + \rho_i)$ . However, in developing eq. (21) we assumed that the transition from punctured section to insulated section is abrupt. Let us examine this assumption more closely.

### 3.2 The transition zone

The cable jacket punctures when and if the transverse voltage at the interface of jacket and shield is higher than some threshold breakdown value. From the definition of  $Y$ , the admittance/length of a transmission line, we may write

$$V = \frac{1}{Y} \frac{\partial I}{\partial x}. \quad (22)$$

For the shield-earth transmission line, we may write [see eq. (3)]

$$\frac{1}{Y} = \frac{1}{Y_i} + \frac{1}{Y_e}, \quad (23)$$

where  $Y_i$  is the admittance of the insulation and  $Y_e$  is an admittance term due to the earth and to the earth-cable interaction. The voltage across the jacket may then be written

$$V_i = V - V_e = \left( \frac{1}{Y} - \frac{1}{Y_e} \right) \frac{\partial I}{\partial x} = \frac{1}{Y_i} \frac{\partial I}{\partial x}.$$

From eq. (1),

$$V_i(x, \omega) = \frac{\Gamma}{Y_i} I(x, \omega). \quad (24)$$

Let us assume that the lightning pulse has somehow managed to penetrate the jacket and enter the shield of the cable, either by induction or by sparking over a lightning protector at a termination, or by actually puncturing the jacket. A short distance from the entry point, the voltage developed across the jacket will be given by (24) with  $\Gamma = \Gamma_I$ . The ratio of  $\Gamma_I$  to  $Y_i$  for standard cable jacket is on the order of  $10^6$  for low frequencies, so  $V_i$  may become quite large. If the current is high enough,  $V_i$  will exceed the breakdown potential of the jacket and an arc will develop. The resistance of the arc is low enough that the current pulse behaves as if it were in direct contact with the earth, that is, as if the cable were bare.

That portion of the current that passes beyond the puncture once again encounters the intact jacket, but the voltage across the jacket does not return abruptly to its breakdown value; if it did, the jacket would be continuously pierced, rather than intermittently punctured. Instead, the voltage builds to its threshold value over some finite distance along the cable. The rate of change of voltage is given by another defining equation of the transmission line

$$\frac{dV}{dx} = ZI \quad (25)$$

where  $Z$  is the impedance/length of the line. For large values of  $I$ ,  $dV/dx$  will also be large and the voltage will build quickly to its breakdown value, at which point the jacket again punctures and current is suddenly able to leak off. As the pulse progresses down the shield, the current decreases,  $dV/dx$  also decreases, and the space between punctures increases. Eventually, the current becomes so small that (24) never reaches the threshold value for  $V_i$  and the jacket remains intact for the remaining length of cable. Douglass<sup>1</sup> has experimentally determined that the minimum value of peak current necessary to puncture the jacket lies between 2000 and 6000 amperes, the latter value pertaining to factory-fresh, carefully buried cable.

While the current is high enough to puncture the jacket, the shield-earth transmission line behaves in the aggregate as if the shield were

in continuous contact with the earth, even though it makes only intermittent contact through tiny pinholes spaced meters apart. As the puncture spacing increases, the behavior of the line approaches that of an insulated cable; eventually  $\Gamma$  assumes the value  $\Gamma_I$ . From the above discussion, it is clear that at no specific point on the cable does behavior change from bare to insulated; indeed, if one were to examine the "bare" cable in detail, it would not appear bare at all. Between the punctures, it is as well insulated as if the punctures did not exist. Only in a macroscopic sense, in which we consider a section of cable that is long with respect to the distance between punctures, can we talk about the cable behaving as if it were bare. As the distance between punctures increases, the scale of this macroscopic dimension becomes larger, until ultimately we talk of the cable being insulated.

The transition from  $\Gamma_B$  to  $\Gamma_I$  is actually quite gradual. The transition from  $Z_{oB}$  to  $Z_{oI}$  is also gradual, and the reflection coefficient will be reduced by some factor depending on how gradual the transition is. As a lower limit we might assume that the transition is so gradual that no current at all is reflected, i.e.,  $\rho_i = 0$ . Equation (21) would then become

$$V_{cs}(0, \omega) = I(0, \omega)Z_s \left[ \frac{1 - e^{-(\Gamma_B + \Gamma_0)x_{th}}}{\Gamma_B + \Gamma_0} + e^{-\Gamma_B x_{th}} \frac{1 - e^{-(\Gamma_I + \Gamma_0)(x_d - x_{th})}}{\Gamma_I + \Gamma_0} \right] \quad (26)$$

Since the attenuation constant for the insulated section of cable is very small (very little current can leak through the intact insulation), the core-shield voltage developed on the insulated portion can be considerable. In fact, for a lightning pulse entering the cable with a value not very much greater than the minimum value needed for puncturing, the insulated portion will be much longer than the punctured portion and the voltage developed will be due almost entirely to the insulated portion. However, if the reflection coefficient is large [eq. (21)], very little current enters the insulated portion and the total voltage at  $x = 0$  will be greatly reduced from the case of no reflection. Hence, the value of the reflection coefficient is critical for estimating the core-shield voltage of the cable; unfortunately, it is impossible to get a good estimate of this value without doing extensive field studies. Since the actual reflection coefficient is unknown, we use eqs. (21) and (26) to bracket the core-shield voltage, with eq. (21) giving the lower limit and eq. (26) the upper limit. Note that in the case of eq. (21), we cannot estimate the lower limits for currents close to the current puncture threshold for, if the peak current is very close to the threshold value, eq. (21) will not hold because the assumption of only a single

reflection in the puncturing portion is not valid if that portion is very short. If the punctured portion is short, the reflected current will not have time to decay before it is again reflected, this time from the assumed infinite impedance termination at  $x = 0$ . Equation (21) is valid only if the puncture region is sufficiently long that only one reflection need be considered.

We now have four expressions for core-shield voltage in standard cable, corresponding to the following combinations of peak current and cable length: eq. (16) for the case in which the current is less than the minimum needed for puncturing, eq. (17) in which the peak current is so great that the cable punctures for its entire length, eq. (21) for the case in which the current is greater than the threshold value and causes the cable to puncture for part of its length, with an assumed sharp transition to the nonpuncturing portion, and eq. (26) for the same combination of current peak value and cable length, but with an assumed gradual transition. Equations (21) and (26) bracket the core-shield voltage for the partial-puncture case. These expressions are summarized in Table I.

#### IV. PROCEDURE

The equations for  $V_{cs}$  developed in Section III require values of  $\Gamma$ , the propagation constant for the shield-earth transmission line, and in one case,  $\rho_i$ , the reflection coefficient for the transition point on a

Table I—Equations used to generate values of core-shield voltage

##### Standard Cable

1.  $I(0, t)_{\text{peak}} < I_{th}$ , jacket does not puncture:

$$V_{cs}(0, \omega) = \frac{I(0, \omega)Z_n}{\Gamma_l + \Gamma_0} [1 - e^{-(\Gamma_l + \Gamma_n)x_d}] \quad (16)$$

2.  $I(0, t)_{\text{peak}} > I_{th}$

A.  $x_{th} > x_d$ , jacket punctures entire length of cable:

$$V_{cs}(0, \omega) = \frac{I(0, \omega)Z_n}{\Gamma_B + \Gamma_0} [1 - e^{-(\Gamma_B + \Gamma_n)x_d}] \quad (17)$$

B.  $x_{th} < x_d$ , jacket punctures part of cable:

i. Reflection at  $x_{th}$ :

$$V_{cs}(0, \omega) = I(0, \omega)Z_n \left\{ \frac{(1 + \rho_i e^{-\Gamma_n x_{th}})(1 - e^{-(\Gamma_B + \Gamma_n)x_{th}})}{\Gamma_B + \Gamma_0} + (1 + \rho_i) \frac{e^{-\Gamma_n x_{th}} [1 - e^{-(\Gamma_l + \Gamma_n)(x_d - x_{th})}]}{\Gamma_l + \Gamma_0} \right\} \quad (21)$$

ii. No reflections at  $x_{th}$ :

$$V_{cs}(0, \omega) = I(0, \omega)Z_n \left[ \frac{1 - e^{-(\Gamma_B + \Gamma_n)x_{th}}}{\Gamma_B + \Gamma_0} + e^{-\Gamma_n x_{th}} \frac{1 - e^{-(\Gamma_l + \Gamma_n)(x_d + x_{th})}}{\Gamma_l + \Gamma_0} \right] \quad (26)$$

partially punctured cable. These values are obtained by solving eq. (11) for  $\Gamma$ , using this solution in eqs. (3) and (4) for  $Y$  and  $Z$ , and then using those solutions in eq. (19) to get  $\rho_i$ . The only difficulty lies in the fact that eq. (11) is a nonlinear, complex transcendental equation whose solution must be obtained numerically for the particular cable and soil parameters of interest.

We have written a computer program that uses Newton's method to solve eq. (11), and with it eqs. (3) and (4). The program has been used to find  $\Gamma$  as a function of frequency for cables of the dimensions and characteristics given in Table II. The resistivity of the jacket was varied while all other parameters of each cable were kept constant; the jacket was assumed to have a resistivity of  $10^{14}$  meter-ohms, corresponding to standard polyethylene,<sup>4</sup> or a resistivity of zero, corresponding to a "bare" cable. The cable parameters and assumed soil parameters are shown in Table II; results for various soil conductivities are shown in Figs. 3, 4, 5, and 6 for the small cable.

The equations for  $V_{cs}$  require several parameters in addition to  $\Gamma$  and  $\rho_i$ . Specifically, we need  $\Gamma_0$ , the propagation constant of the core-shield transmission line;  $Z_s$ , the transfer impedance of the shield;  $I(0, \omega)$ , the frequency spectrum of the lightning pulse where it enters the cable and, in the case of cable which punctures over part of its length,  $x_{th}$ , the assumed point on the cable at which the peak current is reduced to its minimum puncture value,  $I_{th}$ .  $\Gamma_0$  and  $Z_s$  may be computed directly from eqs. (13) and (14);  $I(0, \omega)$  and  $x_{th}$  require the use of Fourier transforms.

We used fast Fourier transform routines to determine  $I(0, \omega)$  from the current pulse  $I(0, t)$ . With current defined every 2.5 microseconds

Table II—Parameters of cable and soil

Cable Parameters		
	Small Cable (25 Pair)	Large Cable (300 Pair)*
Outer Shield Radius, $a_o$	6.6675 mm	31.0896 mm (mean)
Shield Thickness, $t_s$	0.635 mm	0.356 mm
Shield Conductivity, $g_s$	$3.72 \times 10^7$ mho/meter	$2.72 \times 10^7$ mho/meter†
Jacket Outer Radius, $a_{cs}$	7.9375 mm	32.893 mm
Jacket Conductivity, $g_c$	$10^{-14}$ mho/meter	
Jacket Permittivity, $\epsilon_c$	$2.3\epsilon_0$ farad/meter‡	
Cable Depth, $d$	1 meter	
Soil Parameters		
Soil Permittivity, $\epsilon$	$10\epsilon_0$ farad/meter‡	
Soil Resistivity, $\rho$	from 50 to 1000 m- $\Omega$	

\* Sheath of large diameter cable is corrugated, so radius figures represent average values.

† Mean value for steel and aluminum, plus 11 percent due to extra length introduced by corrugation.

‡  $\epsilon_0$  = permittivity of free space =  $8.854 \times 10^{-12}$  farad/meter.

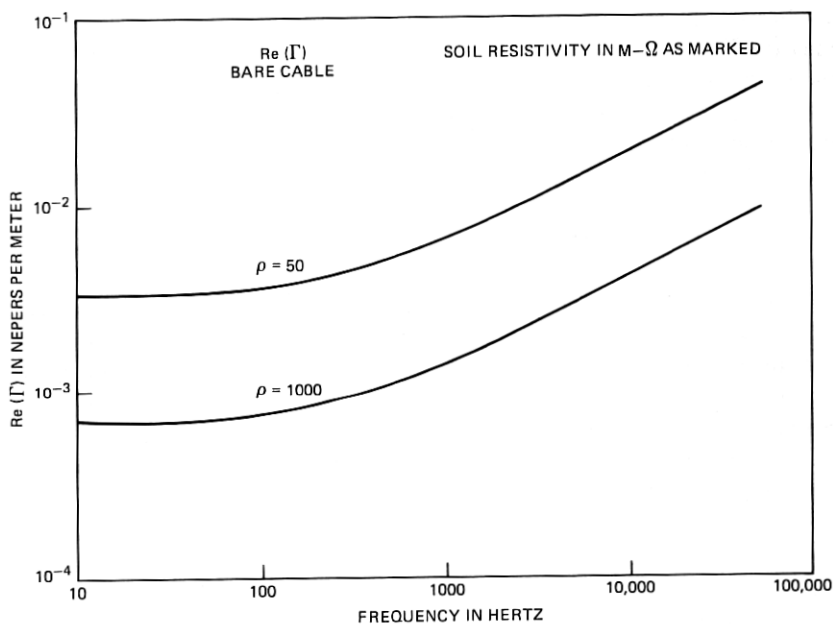


Fig. 3—Real part of  $\Gamma$  for different values of soil resistivity  $\rho$ .

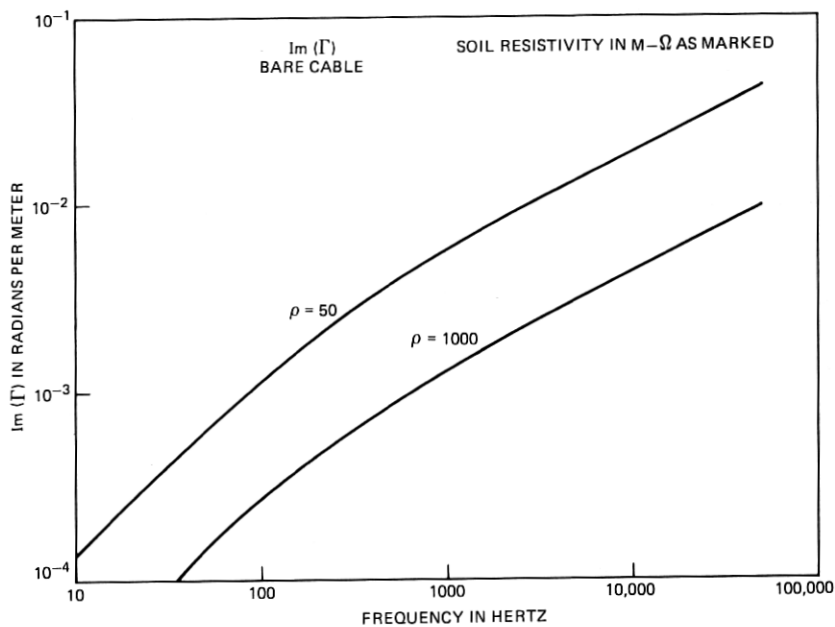


Fig. 4—Imaginary part of  $\Gamma$ .

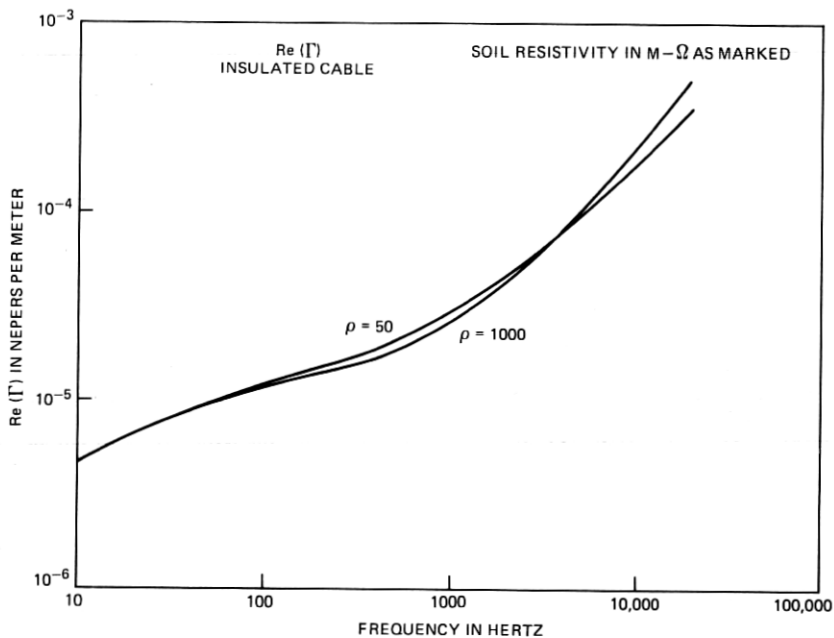


Fig. 5—Real part of  $\Gamma$  for insulated cable.

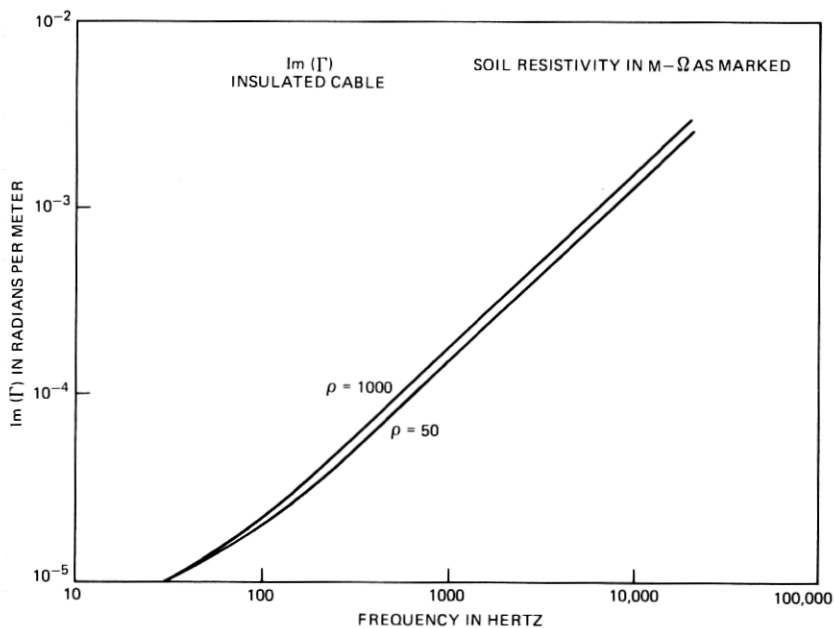


Fig. 6—Imaginary part of  $\Gamma$  for insulated cable.

in the time domain and every 50 Hz in the frequency domain, 8000 points were needed. In one instance, we used a resolution of 10 Hz in the frequency domain, requiring 40,000 points for the transform; the results for the high resolution case differed from those of the low resolution case by less than 3 percent, so we decided to use the 50-Hz resolution for the bulk of the analysis. Thus, the results presented in this paper used a 50-Hz frequency resolution. A typical lightning pulse spectrum is shown in Fig. 7. Notice that the spectrum is rather flat from low frequencies up to about 1000 Hz; it then falls off gradually, eventually attaining a slope of  $1/f^2$  at high frequencies.

Fourier transforms must also be used to find  $x_{th}$ : with  $\Gamma$  set equal to  $\Gamma_B$ , eq. (1) is inverted for different values of  $x$  until that value is found for which the time-domain current pulse has a peak value of  $I_{th}$ . The values of  $x$  used in (1) were determined in practice by a bisection search which located  $x_{th}$  to within 1 meter, requiring 11 inversion operations.

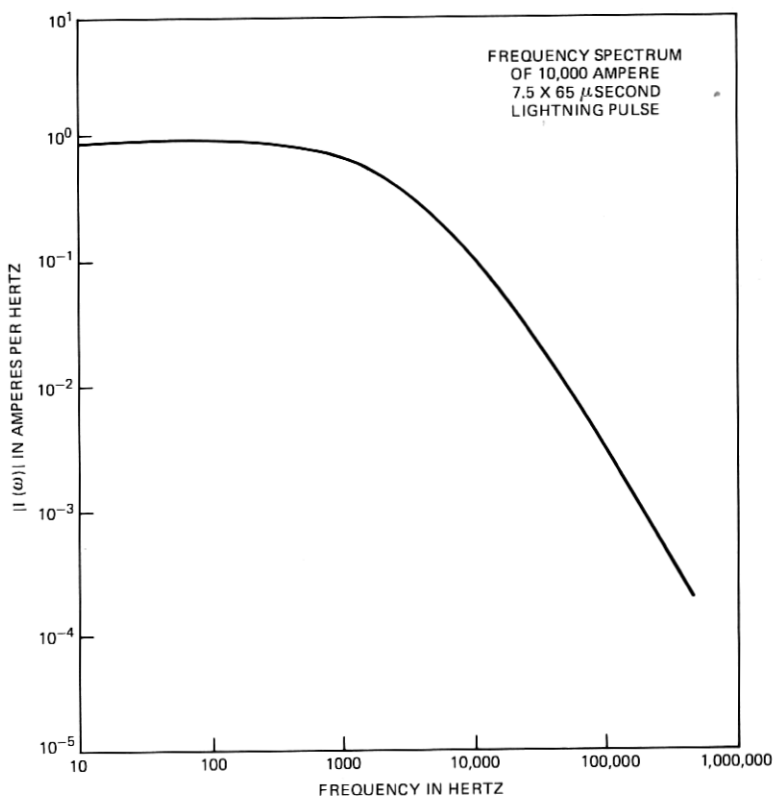


Fig. 7—Lightning spectrum for 10,000 ampere  $7.5 \times 65 \mu s$  pulse.



## V. RESULTS

The equations for  $V_{cs}$  were used to generate profiles of core-shield voltage as a function of peak lightning current for a variety of cable, soil, and pulse parameters. In each case, the cable was assumed to be either uniformly bare or jacketed with standard polyethylene, and the cable length either 100, 1000, or 10,000 meters. In the case of bare cable, eq. (17) was used to generate the core-shield voltage; in the case of the standard jacket, either eq. (16), (17), or (26) was used, depending on the values of  $x_d$ ,  $x_{th}$ , and  $I(0, t)_{peak}$  in accord with Douglass' empirical results; values of  $\Gamma$  correspond to soil conductivities of either 50 meter-ohms (highly conductive) or 1000 meter-ohms (highly resistive); pulse shape was taken as either  $5 \times 40$  (moderately fast) or  $15 \times 65$  (moderately slow).\*

The cable parameters used for most of the cases studied were those of a Bell Laboratories experimental cable being used to measure insulation characteristics. In addition, parameters for a large 300-pair cable were used to investigate the effect of cable size on core-shield voltage (the experimental cable is rather small).

As noted above, for the range of incident lightning currents in which the cable punctures part of its length ( $x_{th} < x_d$ ), eq. (26) which assumed no reflection at the boundary, was used instead of eq. (21), which assumed an abrupt transition and a large reflection coefficient. The reason for not using eq. (21) was simply that it gives essentially the same results as eq. (17) (the "bare" cable core-shield voltage). As described in Section III, in this range of currents we calculate the upper and lower bounds of the core-shield voltages; eq. (26) for the smooth-transition, nonreflecting case gives us the upper bound, and eq. (21) for the abrupt-transition, reflecting case gives the lower bound. However, the lower bound is essentially the bare cable value so, to reduce computation costs, in most cases only the upper bound was calculated separately.

The results we obtained are shown in Figs. 8 to 14, in which we plot the peak value of  $V_{cs}(0, t)$ . A careful examination of Fig. 8 will serve as a guide for the others.

Figure 8 compares core-shield voltage for insulated cable and bare cable for a  $5 \times 40$  pulse, in 1000 meter-ohm soil, with a puncture threshold of 2000 amperes. These parameters represent a fairly typical pulse shape, with representative values for a cable in highly resistive soil. The horizontal axis gives peak current at the point of entry, the vertical axis core-shield voltage at the same point. The horizontal axis

---

\* Although choices of pulse shape were dictated largely by constraints in using the fast Fourier transforms, the waveforms are still good representations of actual lightning currents.

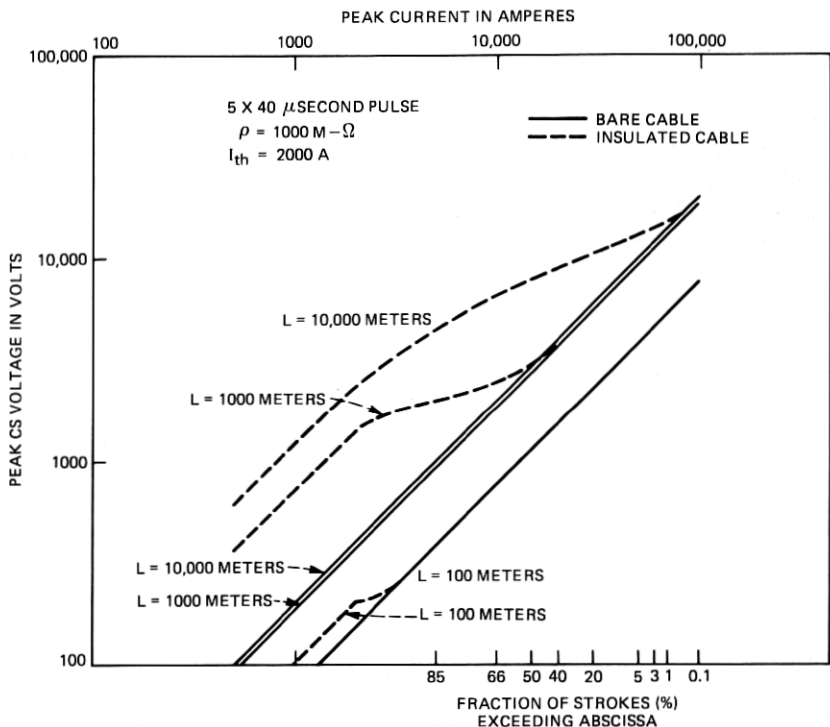


Fig. 8—Core-sheath voltage developed on insulated cable (dashed lines) and bare cable (solid lines), for three different lengths between effectual grounds. Pulse shape  $5 \times 40 \mu s$ , soil resistivity 1000 m-ohms, puncture threshold 2000 amperes. Other parameters are for the small cable (see Table II).

is also graduated in terms of percentile distribution of peak lightning current to buried structure, as estimated by Sunde (Ref. 2, Fig. 9.2). The solid lines give core-shield voltage for bare cable for three different lengths; the dashed lines give voltages for insulated cable, also for the same three lengths.

Let us look in detail at the bare cable values. Note that the results for the three lengths are parallel straight lines. This is consistent with eq. (17) which is linear in  $I(0)$  when  $x_d$  is held fixed. The uneven spacing between the lines illustrates the effect of bare cable's high attenuation constant: The pulse leaks off the shield so effectively that most of it is gone by the time it has traveled 1000 meters, even in high resistivity soil; a cable length of 10,000 meters produces just about the same voltage as a cable 1000 meters long.

For values of peak current less than the threshold value of 2000 amperes, the shape of the curves for insulated cable are similar to those for bare cable. Once again we get three parallel lines correspond-

ing to the three cable lengths. The uneven spacing of the lines again represents the diminishing effect of length as the pulse manages to leak off the shield; the effect is not as pronounced for insulated cable as for bare cable because we are dealing now with a cable with an intact, highly resistive jacket, and almost all the leakage is in the form of displacement current through the capacitor formed by the shield-jacket-earth sandwich. This causes high frequency components of the pulse to be preferentially lost, and the pulse becomes "smeared out" as well as attenuated (see Appendix A).

For current values above the threshold, the results no longer are parallel straight lines. This is the region in which the cable punctures for part of its length and is intact for the remainder. Notice that in each case the slope of the line changes more or less abruptly at the threshold value, the change being less pronounced for the longer cable lengths. Eventually the dashed line converges with the solid line representing the bare cable voltage, since as the peak current increases the cable punctures over a greater percentage of its length and the "bare" term in eq. (26) becomes dominant. The proportion of punctured length to insulated length also explains the change of slope at the threshold value. In all three cases, the cable will puncture for the same length for a given peak current, but this will be a much more significant fraction of the total length for a 100-meter cable than for one 10,000 meters long. Hence, the long cable's voltage changes less abruptly than does the shorter cable's.

From the threshold point at which the jacket begins to puncture to the point at which the dashed line joins the bare cable line, the result shown is the upper limit of the possible core-shield voltage; the lower limit is very close to the solid bare cable line. The actual value of core-shield voltage in this current range will be something between these values, depending on the degree of smoothness of the transition between the punctured and nonpunctured portions of the cable.

Figure 9 shows the results for the same cable and lightning parameters, but with low resistivity soil. The primary effect of lowering the soil resistivity is to make it easier for the current to leak off the shield for both bare cable and the punctured jacket. Since the current now leaks off the punctured jacket more effectively, the polyethylene doesn't puncture as far, and the ratio of punctured to nonpunctured lengths is smaller than for the high-resistivity soil, resulting in a sharper discontinuity at the threshold current point of the graph. All these effects are seen in Fig. 9. Note that the voltages developed by bare cable are smaller than for the high soil resistivity case. The spacing of lines is also much closer because of the diminishing value of extra cable length when the pulse can so easily leave the shield. The lower soil resistivity has a minimal effect over the nonpunctured

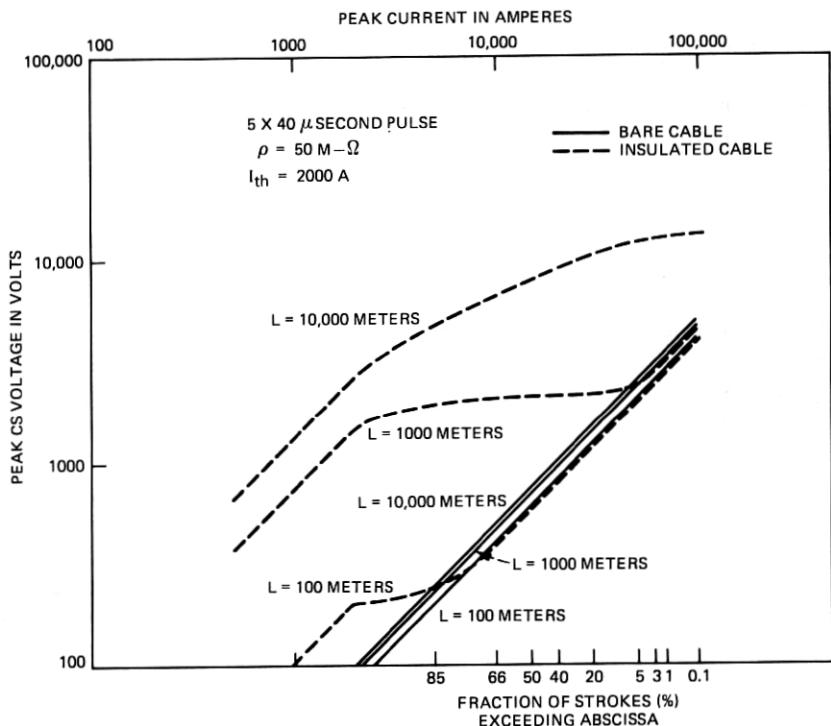


Fig. 9—Same as Fig. 8 with soil resistivity 50 m- $\Omega$ .

region, so those values are not greatly different from the high-resistivity-soil case. These results are for the upper bound of core-shield voltage, and the lower bound will once again be essentially the value for bare cable, so as the soil resistivity decreases the range of values for core-shield voltage becomes greater.

Figures 10 and 11 show the effect of assuming a puncture threshold of 6000 amperes, which is representative of a factory-fresh, carefully buried cable. The straight, parallel-line portion of the standard cable curve has been extended, causing the upper-limit value for the partial-puncturing region to be higher than for the previous cases. The values for the bare cable are, of course, not affected by the choice of puncture threshold, so the lower limit values for the partial-puncturing region remain the same as before. Thus, the range of values for partial puncturing is widened as the puncture threshold increases.

Figure 12 shows the effect of changing pulse shape. In this case, the parameters for the cable and soil are the same as for the case considered in Fig. 8, but now the lightning pulse is slower and wider, with a 15- $\mu$ s rise time and 65- $\mu$ s time to half value. Comparing Figs. 12 and 8,

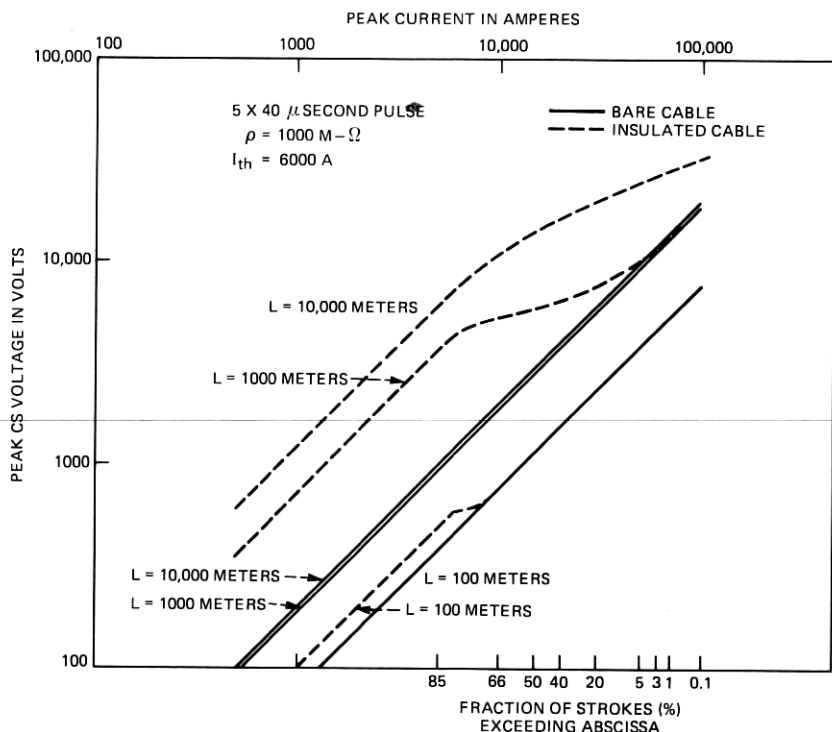


Fig. 10—Same as Fig. 8 with puncture threshold 6000 amperes.

we see that the core-shield voltage is not very sensitive to pulse shape. Sunde (Ref. 2, Chapter 9) contends that, for an infinite cable that punctures its entire length, if both the rise and half times are multiplied by a factor  $k$ , then the core-shield voltage will be increased by a factor  $\sqrt{k}$ . In our case, the ratio of half-times is 65/40, or 1.625, the square root of which is 1.275; the ratio of voltages in Figs. 12 and 8 for the long bare cable is 1.263, which is consistent with Sunde's result, and also supports Sunde's contention that the change of rise time (in our case, a ratio of 3) is less important than the change in fall time.

The effect of cable diameter is seen in Figs. 13 and 14, in which the parameters are the same as for Figs. 8 and 10, but values of  $\Gamma$ ,  $Z_s$ , and  $\rho_i$  were calculated for a large 300-pair cable.

Comparing Fig. 13 to Fig. 8 and Fig. 14 to Fig. 10, we see that the effect of the larger cable is to move the entire set of curves down to lower voltage values. This is due almost entirely to the lower values of transfer impedance for the larger diameter cable, since  $Z_s$  is a linear multiplier for all expressions for  $V_{cs}$ , and  $Z_s$  decreases as the cable shield diameter increases.

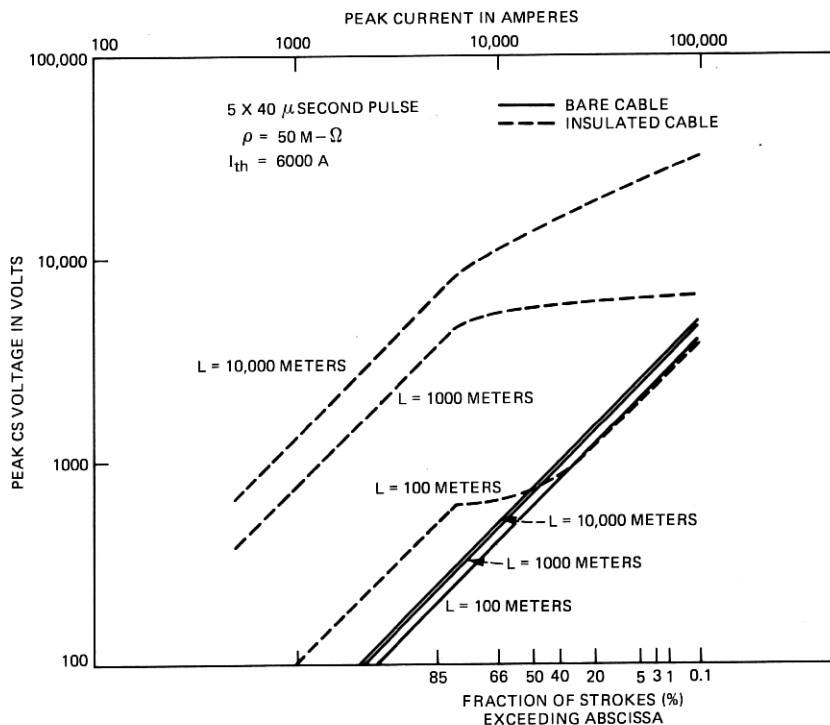


Fig. 11—Same as Fig. 8 with soil resistivity 50 m- $\Omega$  and puncture threshold 6000 amperes.

## VI. INTERPRETATION OF RESULTS

In Figs. 8 through 14, the difference in the core-shield voltage at the stroke point for a given length of bare and insulated cable is the difference between the dashed line and the solid line. Examining Fig. 8, we see that for this rather typical situation the difference is small for all but the longer cable lengths with high peak currents. Using the lower scale that shows probability of attaining a current greater than the given value, we see that, for 50 percent of the expected peak currents, the voltage developed on bare cable equals that developed on insulated cable for lengths up to 1000 meters from the point of entry. Since the cable is assumed to be symmetric about the entry point, this can be interpreted as 2000 meters between effectual grounds (an effectual ground is one that successfully removes most of the current from the shield).

As an example of the use of these figures, let us assume that a core-shield dielectric strength of 10 kV is specified for a telephone plant; for the conditions of Fig. 8, about 25 percent of lightning strokes may generate a peak core-shield voltage *greater* than 10 kV on insulated

cable. Assuming a bare cable model reduces this to all but the largest 5 percent of lightning strokes. The values derived for insulated cable are maximum values and assume no reflection at the interface between punctured and nonpunctured regions of the cable. The values actually developed on the insulated cable will probably be somewhat less than that indicated in the figure, although from the argument of Section III it would seem that the true values should be closer to the upper limit, as indicated by the dashed line, than to the lower limit, which is essentially the bare voltage.

Figure 9 shows that the difference in core-shield voltage is much more dramatic for low resistivity soils, even for cables of shorter length. In the case of a very long distance between effectual grounds, the bare cable assumption produces a distinct underestimation. However, the voltage developed in low resistivity soil, even on insulated cable, is much lower than that developed in high resistivity soil (Fig. 8), so the voltage difference, while considerable, may not be significant.

Figures 10 and 11 show that, for cable which requires 6000 amperes to puncture the outer jacket, the bare cable assumption again provides a substantial underestimation of voltage for the 10-km cable length.

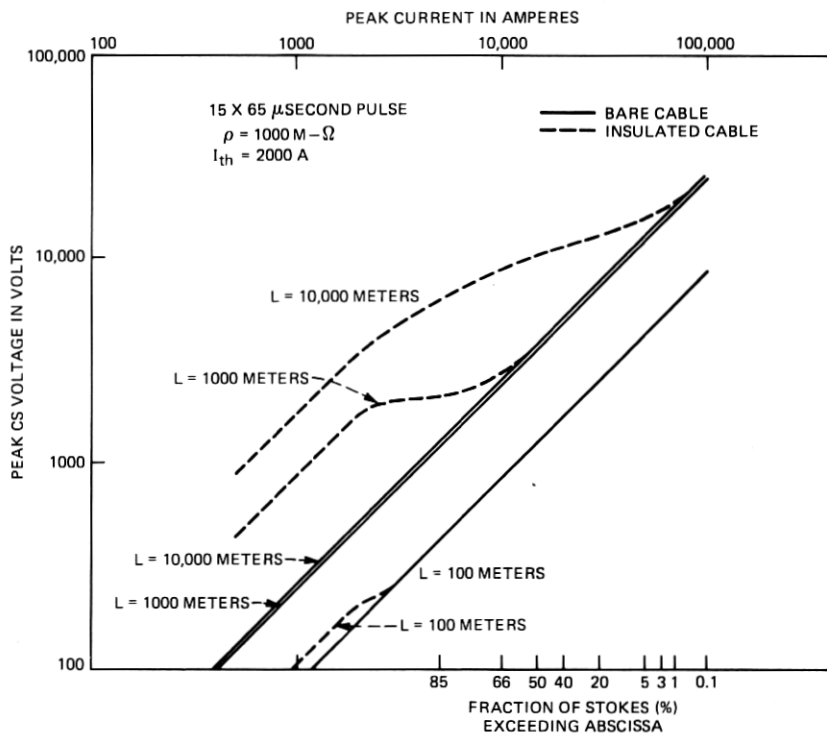


Fig. 12—Same as Fig. 8 with pulse shape  $15 \times 65 \mu\text{s}$ .

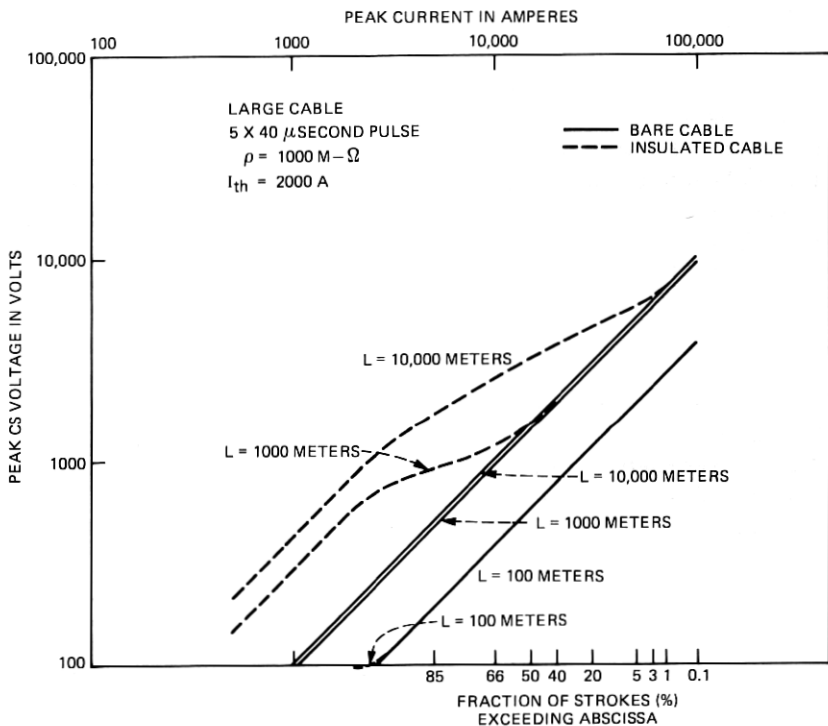


Fig. 13—Same as Fig. 8 with parameters calculated for large cable (see Table II).

Using our 10-kV example, Fig. 10 shows that, in the case of high resistivity soil, 68 percent of the lightning strokes will produce core-shield voltages greater than 10 kV on insulated cable, as opposed to 5 percent of the strokes on bare cable; for low resistivity soil (Fig. 11), the comparable figures are 68 percent for insulated cable and less than 0.1 percent for bare cable.

## VII. DISCUSSION

It would be helpful to examine some of the assumptions inherent in the model that we have developed to interpret properly the results presented in this paper. The theoretical basis for most of this work is the transmission line model of Sunde.<sup>2</sup> We have found it necessary to make two major modifications of Sunde's development: First, Sunde assumed that the cable jacket would be uniform over the length of the cable, while we have assumed that the jacket punctures over part of its length. Second, Sunde assumed that his cable was infinitely long, while we have postulated "effectual grounds" that serve to terminate the cable at some finite length.



We have presented a lengthy discussion in Part III on the implications of the jacket puncturing part of its length; a word should be said about the assumption that the jacket punctures at all. It seems to have been accepted wisdom as far back as 1945 that lightning on a cable shield escapes by forming pinholes in the cable jacket;<sup>5</sup> some authors have reported seeing pinholes in lightning-damaged cables.<sup>6,7</sup> Douglass<sup>1</sup> reported seeing pinholes in the insulation of a buried wire that had been surged with artificial lightning. The insulation was a light gray, and the pinholes had shown up as tiny black dots; however, Douglass was unable to find any pinholes on the dark gray jacket of a buried cable that had also been surged with artificial lightning.

If the reader chooses not to accept the pinholing mechanism, the model we have developed is not greatly impaired, so long as he is willing to accept Douglass' observation that, whatever the mechanism, a buried cable stressed with a current pulse whose peak value exceeds some threshold permits the pulse to propagate approximately as if the cable were bare rather than insulated. Accepting the pinholing mechanism does make it easier to postulate the characteristics of the cable

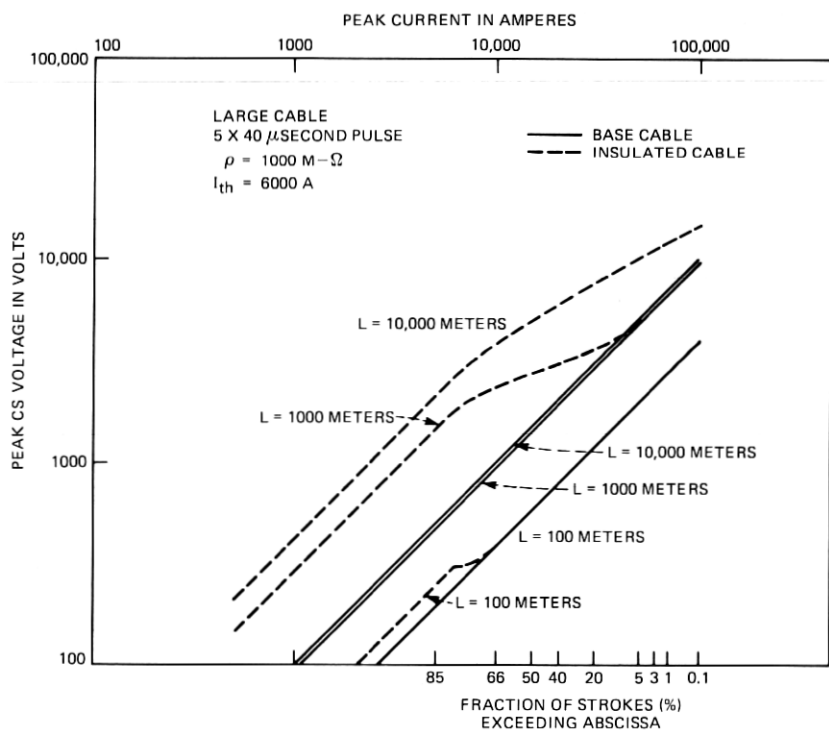


Fig. 14—Same as Fig. 8 with parameters calculated for large cable and puncture threshold 6000 amperes.

in the vicinity of the "bare"-insulated transition zone. If the pinholing hypothesis is rejected, some other mechanism would have to be proposed to discuss the effect of a possible transition zone on pulse propagation.

Our second assumption is that the cable we are considering is terminated at some length in an "effectual ground," which is a ground that serves to remove most of the current from the shield. From transmission line theory, such a ground has an impedance equal to the characteristic impedance of the shield-earth transmission line, which for a small diameter cable in 1000 meter-ohm soil is about 40 ohms with an angle on the order of  $-7$  degrees. A ground which differs from this will remove only part of the current, the remaining current being reflected back along the line as a positive current wave if the termination impedance is less than  $Z_0$  and as a negative current wave if the termination impedance is greater than  $Z_0$ . These current waves will produce core-shield voltages at  $x = 0$  of the same sense as the wave itself. Thus, a cable terminated in a reflection-producing ground will produce a second voltage wave at the origin, which may be of the same sense or a different sense from the original wave. The further the termination is from the origin, the less likely it is that the second wave (which is always smaller in magnitude than the primary wave because of the attenuation of the line) will affect the peak value of  $V_{cs}$ .

The above discussion assumes that the cable actually terminates in a ground connection. A more likely configuration is that the cable is grounded at several points along its length. In that case, the impedance seen by the current as it approaches the ground connection is the parallel combination of the ground impedance and the impedance of the remaining length of cable. Depending on whether this combination is greater than or less than the characteristic impedance of the shield-earth transmission line, a negative or positive current wave will be reflected back to the origin. That portion of the pulse which is not reflected will be divided between the ground connection and the remainder of the line, in inverse proportion to their impedances. The more the ground impedance differs from the characteristic impedance, the greater the proportion of current that is either reflected or transmitted rather than removed to earth. With this configuration, it is impossible to remove all the current with a single ground—the most that could be removed at any one point would be half the remaining current. The implication of this is that when we speak of a cable length of, say, 1000 meters, what this means is that by the time the current gets 1000 meters away from the entry point it has encountered enough grounds of sufficient quality that just about all the current has been removed.

For this reason, it is essential that the reader interpret the curves of

Figs. 8 to 14 properly: the different cable lengths indicated on the curves are lengths to an *effectual ground*; in plant with good grounds, this may be less than the physical length of the cable; in plant with poor grounds, this may be considerably longer than the actual distance between grounds. If bonds are available to a power system multi-grounded neutral, a typical ground impedance may be on the order of 5 ohms; in high resistivity soil, a single ground rod may have an impedance of several hundred ohms. Thus, the character of the plant must be taken into account when interpreting the curves of Figs. 8 through 14.

Implicit in this idea of an effectual ground is the assumption that reflections from the intermediate and final terminations may be neglected in calculating the core-shield voltage. These reflections will not make a significant contribution to the peak voltage at the entry point of the pulse if one or both of the following conditions exist: (i) The attenuation of the line is so great that the reflected wave is very much smaller in amplitude than the incident wave; or (ii) the line is so long that the reflected wave arrives with sufficient delay that it does not contribute to the peak voltage developed by the incident wave, but rather adds its peak to the tail of the incident voltage wave, producing either a double-peaked or smeared-out voltage.

In the case of a bare cable or an insulated cable that punctures its entire length, the attenuation on the shield-earth transmission line is very large, on the order of  $10^{-2}$  neper/meter. The reflected wave, even on a cable as short as 100 meters, would be at most  $0.37\rho_i$  times the peak value of the incident wave, and by the time it returned to the entry point it would be on the order of  $0.1\rho_i$  times the incident wave, where  $\rho_i$  is the reflection coefficient of the termination as defined in eq. (19), with  $Z_0$  taken to be the termination impedance. Thus, in the very important cases of a bare cable or a cable punctured over its entire length, unless the cable is very short reflections will make a small contribution to the peak core-shield voltage.

In the case of an insulated cable in which the jacket punctures part of its length or not at all, we must be a bit more cautious. In the case of a cable punctured over a portion of its length, we have considered the case of reflections from the punctured-intact transition zone in Section III. In the case of a cable in which the lightning pulse is initially less than the assumed puncture threshold of the jacket, the attenuation constant of the shield-earth transmission line will be very small, and the peak core-shield voltage would be changed by a factor of  $1 + k\rho_i$ , where the factor  $k$  is largely a function of the cable length. For a length on the order of 100 meters, the reflected wave will be very nearly in-phase with the incident wave, and  $k$  will have a value of very close to 1. In this case, reflections from a very low impedance termi-

nation, such as a power-system multigrounded neutral, could increase the core-shield voltage by a factor of nearly  $1 + \rho_i$ . Since the maximum value of  $\rho_i$  is 1, this would have the effect of shifting upward by at most a factor of 2 the straight-line portion and the immediately adjacent transition-zone portion of the  $L = 100$  meter curve for insulated cable in Figs. 8 through 14. Alternatively, if we interpret the curves in terms of distance to effectual grounds, a 50-meter length of cable terminated in a perfect short to remote earth would have an effective length of 100 meters, so the straight-line portion of the 100-meter curve would represent a cable somewhat longer than 50 meters, terminated in, say, a power-system multigrounded neutral with impedance to remote earth of about 5 ohms.

As the cable length increases, the reflected wave takes longer to reach the origin, and "falls behind" the incident wave. This has the effect of reducing the factor  $k$  in the expression  $1 + k \rho_i$ . For the small diameter cable,  $k = 0.63$  for a cable length of 1 kilometer, 0.47 for a cable length of 5 kilometers, and 0.36 for a cable length of 10 kilometers. For the example mentioned above of a very-low-impedance ground, the straight-line portion of the  $L = 1000$  meter curve in Figs. 8 through 14 would be shifted up by at most a factor of 1.63, and the corresponding portion of the  $L = 10,000$ -meter curve by at most a factor of 1.36. Thus, the straight-line portion of the 1000-meter curve could be interpreted as representing a cable a little longer than  $1000/1.63 = 613$  meters, terminated in a power-system multigrounded neutral, and the straight-line portion of the 10,000-meter curve as representing a cable a little longer than  $10,000/1.36 = 7353$  meters, terminated in a power-system multigrounded neutral.

### VIII. CONCLUSIONS

In this paper, we have calculated the voltage developed between the core and the shield of a buried cable when a lightning pulse travels down the shield, by modeling the cable as a pair of coupled transmission lines in which the coupling parameter is the shield transfer impedance. We have included the effect of the cable jacket puncturing under the stress of the lightning current. For the portion of the cable in which puncturing takes place, the shield-earth transmission line has a propagation constant typical of a bare shield; for the remainder of the cable the propagation constant is that of an insulated shield.

This nonlinear behavior of the cable jacket generally results in higher core-shield voltages than would be predicted by using a bare-shield model. We have found in particular that, for small-diameter cable and long distances between good grounds, the bare-shield model produces voltages substantially lower than those predicted when the partial-puncturing of the jacket is taken into account.

## APPENDIX A

### *Samples of Core-Shield Voltage Waveforms*

In the analysis presented in this paper, we are interested in the peak value of core-shield voltage developed on cable when a lightning pulse travels down the cable shield. Since the lightning current is a function of time, the core-shield voltage is also a function of time. In the course of developing our computer programs, we found it useful to examine the  $V_{cs}$  waveforms to assure that the results were physically meaningful and the programs were developing properly. A sample of these waveforms are presented here. In each of the figures the current waveform is shown as a dotted line, with reference to the left-hand scale; three voltage waveforms corresponding to three different cable lengths are shown as solid lines, with reference to the right-hand scale. The horizontal axis is time, and is the same in all the figures.

In Fig. 15, we have typical  $V_{cs}$  curves for bare cable. The current has a peak value of 500 amperes but, because of the nature of the response (peak  $V_{cs}$  is a linear function of peak current), with proper adjustment of the axes the same set of curves would be obtained for any input current. Note that the peak value of voltage comes some time after the current has reached its peak value, and that the voltage fall time

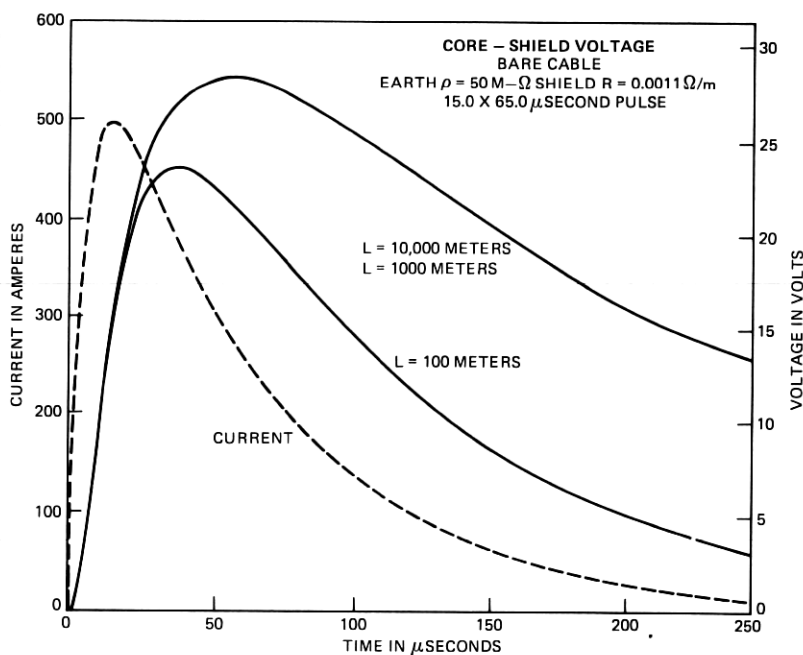


Fig. 15—Input current pulse and core-shield voltage waveforms for bare cable. Peak input current = 500 amperes.

is also much longer than that of the current. The shield-earth transmission line is acting as a low-pass filter, removing high-frequency components and accentuating low-frequency effects; the voltage curves are softer, "smeared-out" versions of the current waveform. This is generally true for all the figures. Note also that the peak occurs earlier for the short line (100 meters long) than it does for the longer lines (1000 and 10,000 meters), and in fact that the latter curves are so similar as to be indistinguishable in the figure. The longer time to reach peak value for the longer lines is due to the fact that a greater proportion of high-frequency components have been removed over the longer lengths; the similarity between the two waveforms indicates that, with bare cable's high attenuation rate, most of the current has been removed by the time the pulse travels 1000 meters, and that increasing the cable length by an order of magnitude has relatively little effect.

The remaining figures show  $V_{cs}$  waveforms for insulated cable. Earth resistivity is taken as 50 meter-ohms, and the threshold value for puncturing is 2000 amperes. It is assumed that there is no reflection from the transition region.

Figure 16 shows the voltage developed with a peak input current of

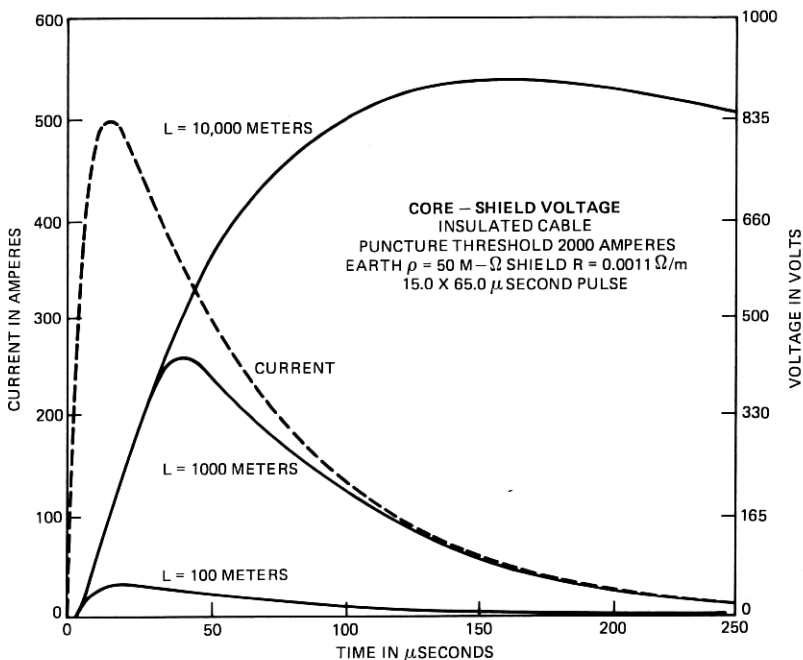


Fig. 16—Input current pulse and core-shield voltage waveforms for insulated polyethylene-jacketed cable. Peak input current = 500 amperes, threshold current  $I_{th} = 2000$  amperes, input waveform  $15 \times 65 \mu s$ .

500 amperes, which is below the threshold value, so the cable acts as if it were insulated over its entire length. The waveforms are qualitatively different from those of the bare cable in Fig. 15. The intact insulation results in a very low attenuation rate for the current, and the effect of increasing the cable length is considerable. Note that the voltage scale in this case is two orders of magnitude greater than it was in Fig. 15. The smearing-out effect becomes even more pronounced, especially for the long cable length. The fall times are less distorted than the rise times, since in a crude way we can think of the fall times as being governed by the low-frequency components of the current pulse, and the low-frequency components are not attenuated as much as the high-frequency components.

The parameters for Fig. 17 are the same as for Fig. 16, except that the input pulse has a faster rise and fall time. The curves in the two figures are very similar, illustrating the very minor effect of current waveform in this study.

In Figure 18, we are back to the longer input pulse. The peak current is now 5000 amperes, which is above the threshold value, so the cables are puncturing at least part of the way. The voltage waveforms are now more complex than before, although at first glance they seem to

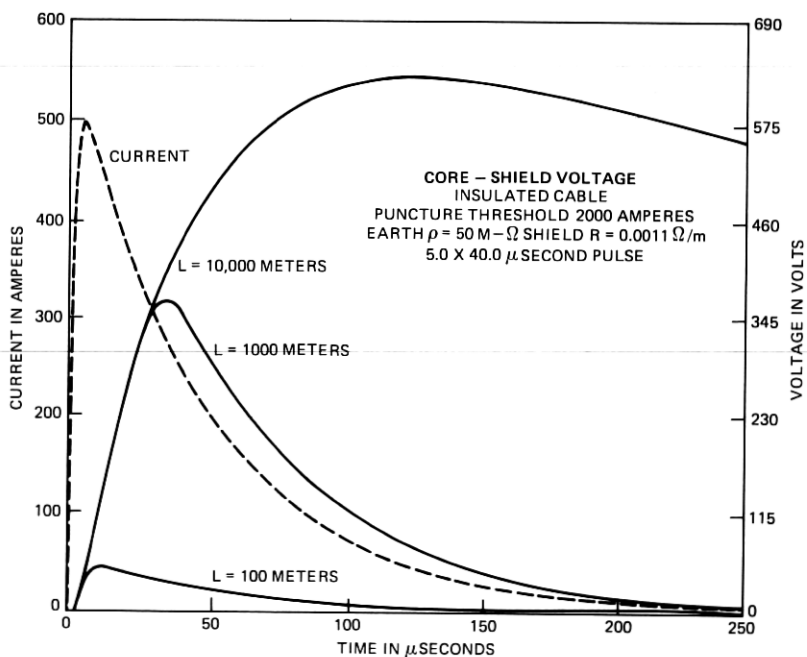


Fig. 17—Same as Fig. 16, but the input current waveform is a sharper pulse,  $5 \times 50 \mu\text{s}$ . Notice the similarity of the voltage waveforms to those of Fig. 16.

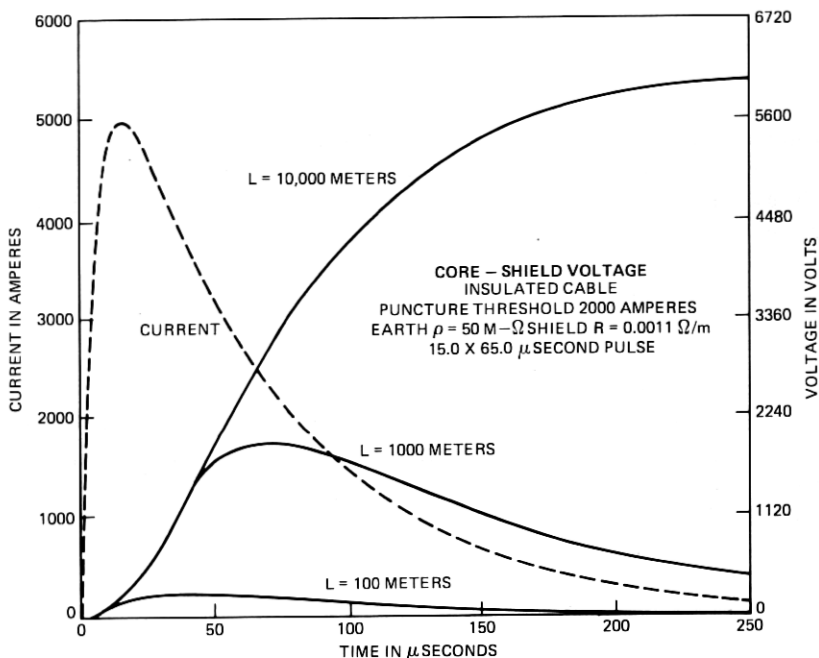


Fig. 18—Same as Fig. 16, but peak input current = 5000 amperes.

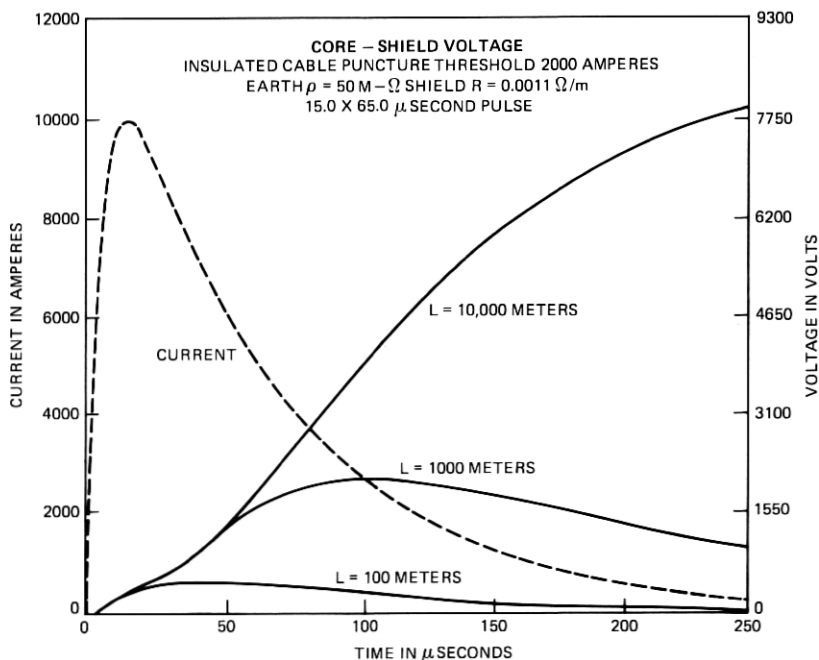


Fig. 19—Same as Fig. 16, but peak input current = 10,000 amperes.



be almost identical to those of Fig. 16. With the cable puncturing part of the way, there will be one component of the voltage due to the punctured part, and another component due to the intact portion. Since the current must pass through the punctured portion before it reaches the intact portion, the voltage developed by the latter will appear later than that of the former, so we are seeing two voltage waves in each curve, the earlier (and smaller) one due to the punctured region, the later and in general larger one due to the insulated region. With a peak input current of 5000 amperes, the punctured region is not very long, and the insulated portion dominates the waveform. However, the effect of the punctured region can be seen near the origin, where the voltage curves start off with a very small slope, and then start to climb quickly. This slow initial rise is not present in Fig. 16 and is due to the fact that on the scale of this figure the initial voltage due to the punctured region appears very small.

In Figs. 19 and 20, the input current increases to 10,000 and 20,000 amperes. As the peak current increases, the length of the punctured region also increases, and the contribution of the punctured zone rises. In Fig. 19, we see the formation of an inflection point as the voltage curve begins to separate clearly into two parts; in Fig. 20, the contributions of the two zones are becoming equal for the middle curve. Meanwhile, the peak due to the intact zone is seen to move further off

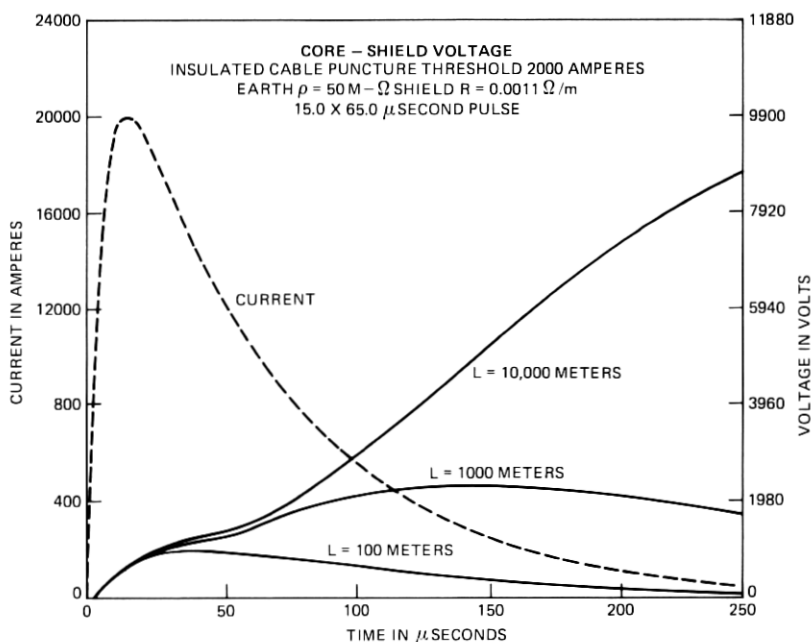


Fig. 20—Same as Fig. 16, but peak input current = 20,000 amperes.

to the right—for the longest cable it has moved entirely off scale. Plots for higher input currents, if carried out for longer time scales, would show a double peak emerging for the 10,000-meter cable, with the first peak slowly becoming predominant. In all cases, when the first peak (representing the punctured region) exceeds the second peak (representing the intact region), the peak voltage developed by the insulated cable becomes the same as the peak voltage developed by bare cable, and the dashed and solid curves of Figs. 8 to 14 of the text converge.

## REFERENCES

1. D. A. Douglass, "Lightning Induced Current Surges on a Buried Multicoaxial Cable System," *Wire and Cable Proceedings*, 1971.
2. E. D. Sunde, *Earth Conduction Effects in Transmission Systems*, New York: Dover, 1968.
3. S. A. Schelkunoff, "The Electromagnetic Theory of Coaxial Transmission Lines and Cylindrical Shields," *B.S.T.J.*, 13, October 1934, pp. 532-579.
4. F. M. Clark, *Insulating Materials for Design and Engineering Practice*, New York: John Wiley, 1962, p. 469.
5. E. D. Sunde, "Lightning Protection of Buried Toll Cable," *B.S.T.J.*, 24, No. 2 (April 1945), pp. 253-300.
6. G. J. Crowdes and C. L. Dawes, "An Analysis of Pinhole Punctures in Underground Cable Jackets," *Electrical Engineering*, May 1961, pp. 355-357.
7. U. P. Ronald, "Conductive Plastic Sheath on Buried Communication Cable for Reduced Lightning Damage," *IEEE International Conference on Communications*, Philadelphia, Pa., June 19-21, 1972, paper 35-7.